CALCULATIONS FOR A MERCURY JET TARGET IN A SOLENOID MAGNET CAPTURE SYSTEM

J. Gallardo, S. Kahn, R. B. Palmer, P. Thieberger, R. J. Weggel, BNL, Upton, NY 11973
K. McDonald, Princeton University, Princeton, NJ 08544

Abstract

A mercury jet is being considered as the production target for a muon storage ring facility to produce an intense neutrino beam. A 20 T solenoid magnet that captures pions for muon production surrounds the mercury target. As the liquid metal jet enters or exits the field eddy currents are induced. We calculate the effects that a liquid metal jet experiences in entering and exiting the magnetic field for the magnetic configuration considered in the Neutrino Factory Feasibility Study II

1. INTRODUCTION

A liquid mercury jet is chosen for the target for the Neutrino Factory Feasibility Study II [1]. A high Z material is desirable because the pion production cross-section grows as Z^2. However the intense proton beam would melt a target made of a solid high Z material. A target system using mercury could recycle the spent target. Mercury moving in a magnetic field experiences induced eddy currents. These induced currents cause the jet to experience retarding and compressive forces upon entry into the field and further retarding forces and negative hydrostatic pressure upon exiting the field. The negative pressure may cause cavitations in the mercury jet. The purpose of this study is to calculate the lowest order effects of a liquid metal target moving in a solenoid magnetic field. This paper is based in part on previous calculations performed [2,3]. Another study of the magnetohydrodynamics of a mercury jet entering a solenoid magnetic field using the FronTier code [4] has been done.

This study looks at the induced azimuthal current and the associated axial and radial forces and hydrostatic pressures. The axial forces retard the mercury jet and produce transverse forces and deflections. In addition there are axial currents induced if the jet axis does not coincide with the magnetic field axis. These axial currents produce transverse elliptical distortions of the mercury jet, which we estimate. Formulae for these effects are given in section 2. In section 3 the magnetic system for the pion capture system is described and from the calculated fields we provide numerical estimates of the magneto-hydrodynamic effects. Section 4 uses the results from the calculation of the axial velocities in section 3 as input for a finite element calculation to obtain the induced axial fields. This permits the calculation of the elliptical distortion of the jet.

2. FORMULAE

One can obtain insight into the dynamics of a mercury jet moving in a magnetic field from low order calculations. In these calculations one assumes that the eddy currents in the jet do not significantly perturb the magnetic field. Since the electrical resistivity of mercury is large, the skin depth is much larger than the radius of the jet and the mercury does not shield the magnetic field. In addition, changes in the size, shape and trajectory of the jet are small. The calculations will show that these assumptions are valid. The angle of inclination between the jet and the solenoid field axis is sufficiently small that one can make the near axis field approximations.

2.1 Axial Forces

Faraday's law can be used to obtain the azimuthal current density from changing $B_{z'}$, where $B_{z'}$ is the axial field in the local coordinate system of the Hg jet:

$$j_\phi \approx \frac{rv\kappa}{2}\frac{dB_{z'}}{dz'} \tag{1}$$

where κ is the conductivity of the mercury and v is the velocity of the jet. There are three contributions to the axial force density associated to $j_{\phi'}$. There is an axial retarding force that comes directly from the field acting on the induced current:

$$f_{z'}(direct) = j_\phi B_r = -\frac{r^2}{4}v\kappa\left(\frac{dB_z}{dz}\right)^2 \tag{2}$$

where $B_r \approx -\frac{r}{2}\frac{dB_z}{dz}$. Upon entering a magnetic field there is a radial inward force density $f_r = j_\phi B_{z'}$ which produces a hydrostatic pressure that will exert an axial pressure that must be added to the direct axial force:

$$f_z(hydrostatic) = -\left(\frac{r_o^2 - r^2}{4}\right)v\kappa\frac{d}{dz}\left(B_z\frac{dB_z}{dz}\right) \tag{3}$$

where r_o is the radius of the mercury jet. As the mercury jet leaves the field, the radial force is outward and can possibly cause the mercury to cavitate and break up. There is an additional shear force density $f_{z'}^{shear} = -B_y j_\phi \sin\phi$:

$$f_z(shear) = \frac{rv\kappa}{2}B_y\frac{dB_{z'}}{dz'}\sin\phi \tag{4}$$

This force has an opposite sign on the top and bottom of the jet. The total force density is the sum of these three forces and varies with r′:

$$f_{z'}^{Total}(r,z) = f_{z'}^{direct} + f_{z'}^{hydrostatic} + f_{z'}^{shear} \tag{5}$$

The average force density integrated over the jet cross section is

$$\langle f_z \rangle \approx \frac{r_o^{\,2}}{8} v\kappa \left[\left(\frac{dB_{z'}}{dz'} \right)^2 + \frac{d}{dz'} \left(B_{z'} \frac{dB_{z'}}{dz'} \right) \right] \quad (6)$$

These forces will decelerate or accelerate different layers of the mercury liquid, providing different velocities in these layers. The change in velocity at different *r* and *z* can be obtained by integrating the acceleration along the Hg jet path:

$$\Delta v(r,z) = \int_{z_o}^{z} f_z^{\,total}(r,\xi) \frac{1}{v(r,\xi)\rho} d\xi \quad (7)$$

where ρ is the density of mercury. As the jet decelerates, the radius of the jet increases to compensate the accumulation of the mercury, since the liquid is incompressible. The radius as a function of z is

$$r(z') = r_o \left(1 - \frac{\langle \Delta v(z') \rangle}{v} \right) \quad (8)$$

2.2 *Transverse Deflections*

The vertical force can be obtained by integrating the vertical component of the radial force.

$$\frac{dF_{y'}}{dz'} = \frac{\pi}{8} v\kappa r^4 \frac{dB_{z'}}{dy} \frac{dB_{z'}}{dz} \quad (9)$$

The angular deflection can be obtained by integrating

$$\theta(z') = \int_{z_o}^{z} \frac{1}{\pi\rho v^2 r^2} \frac{dF_y}{d\xi} d\xi = \frac{\kappa r^2}{8\rho} \int_{z_o}^{z} \frac{1}{v} \frac{dB_z}{d\xi} \frac{dB_y}{d\xi} d\xi \quad (10)$$

along the jet path. A second integration can give the displacement of the mercury jet from the nominal path.

2.3 *Axial Eddy Currents and Elliptical Distortions*

The transverse component of the magnetic field, B_y, also varies along the trajectory of the mercury jet. It can be shown that the axial current density, j_z, can be related to the changing B_y by $j_z = xv\kappa \, dB_y/dz'$ where *x* is the transverse horizontal position. These axial currents produce a magnetic horizontal force density:

$$f_x(magnetic) = xv\kappa B_{y'} \frac{dB_{y'}}{dz'} \quad (11)$$

This force will be balanced by a restoring force from the surface tension of the mercury, and with the added condition that the mercury acts as an incompressible liquid, will produce an elliptic deformation of the mercury jet. This is discussed in reference [2].

3. CAPTURE SYSTEM

Figure 1 shows the geometry of the solenoid magnet capture system used in the Neutrino Factory Feasibility Study II in the vicinity of the target. A 20 T solenoid magnet surrounds the mercury jet target. Downstream the field drops off to 1.25 T in 18 meters. The inner coils surrounding the target are warm hollow-conductor coils, and the outer coils are superconducting. There is a high permeability steel pole in the field to shape the field. This pole will be highly saturated and will provide a nozzle for the mercury jet. It will permit the mercury jet to be guided as it enters the rapidly varying part of the field.

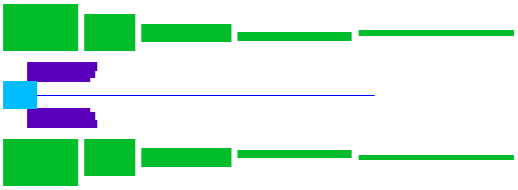

Figure 1: Sketch of the solenoid magnet system around the target. The dark blue rectangles indicate the warm inner coils and the green rectangles indicate the surrounding superconducting coils. The turquoise rectangle is a high magnetization steel pole.

Table 1: Parameters describing the solenoid coils used in the target capture system.

Coil	$Z_{central}$	Half-Width	R_{inner}	R_{outer}	J
	cm	cm	cm	cm	kA/cm^2
HC1	-29.35	42.75	18.00	23.43	2.796
HC2	-26.3	45.8	23.43	34.01	2.01
HC3	-25.05	47.05	34.01	44.19	1.475
SC1	-54.4	50.3	60.45	123.97	2.808
SC2	40.1	34.2	60.45	109.98	2.809
SC3	144.75	60.45	73.53	97.03	3.011
SC4	292.25	77.05	74.95	85.33	4.278
SC5	484.65	105.35	82.00	88.40	5.323

The mercury jet follows a trajectory that is 67 mrad off the solenoid axis, so that pions that are produced in the target are not reabsorbed in the target after one Lamor revolution. The 24 GeV proton beam is inserted into the solenoid 33 mrad off the solenoid axis, so that the neutrals do not travel straight down the beam-pipe. The mercury jet is chosen to have a radius of 0.5 cm so as to contain the transverse size of the proton beam

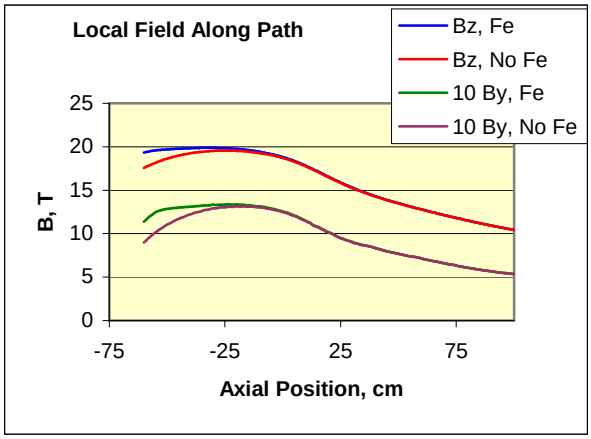

Figure 2: B_z and B_y are given as a function of the path position in the local coordinate system of the mercury jet. Curves show the field with and without the presence of a steel pole. The B_y curve is multiplied by 10 to be visible on the plot.

Figure 2 shows the axial component of the magnetic field in local coordinates along the path of the mercury jet from the end of to pole to a place well beyond the interaction of the jet with the proton beam. The figure shows a comparison of the field with and without the pole to illustrate that the pole flattens $B_{z'}$ in the target region.

Figure 2 also shows the vertical transverse local field $B_{y'}$ (multiplied by 10 to be visible) along the same path. A finite element program is generally not accurate enough to obtain derivatives of the fields, since the field potential varies only quadratically within the element. In order to obtain the derivatives $dB_{z'}/dz'$ and $dB_{y'}/dz'$, we fitted $B_{z'}$ and $B_{y'}$ with a 6th order polynomial to the curves in Fig. 2.

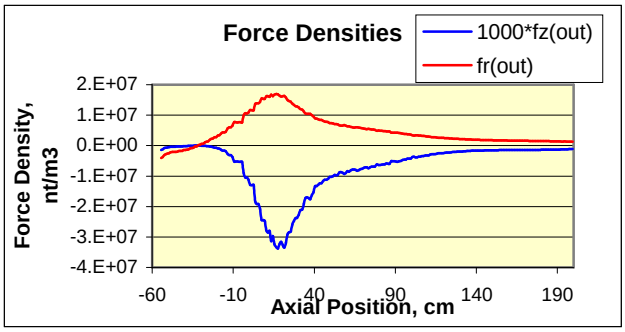

Figure 3: Force densities f_z and f_r on the outer surface of the mercury jet. F_z includes the direct contribution and the hydrostatic contribution.

Figure 3 shows the force densities calculated from equations in Sec. 2; f_z and f_r are calculated on the outer surface of the mercury jet (f_z includes both the direct contribution from $j_\phi B_r$ and the axial hydrostatic pressure from the radial force). The axial force causes a retardation of the jet entering the field. Figure 4 shows the reduction of the velocity as a function of the axial position. The figure shows separately the direct $j_\phi B_r$ contribution and the hydrostatic contribution along with the total reduction.

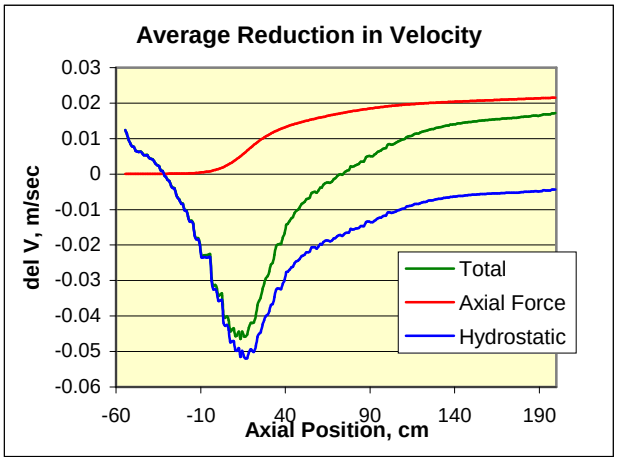

Figure 4: Average reduction in the mercury velocity as a function of the path position. The direct axial force contribution (red), the hydrostatic axial contribution (blue) and the total (green) are shown.

There is a shear component to the axial force that comes from $j_\phi B_y$. This force has the effect of accelerating one half of the jet while retarding the other half. The effect can be potentially disruptive. It can be controlled by minimizing the incline angle of the mercury jet so that B_y is small (we have chosen 67 mrad), minimizing the radius of the jet (since this effect varies as r^3), and by minimizing dB_z/dz which is done using the high magnetisztion pole in the solenoid.

The transverse angular deflection and a transverse displacement of the jet can be obtained from the transverse vertical force using equations in Sec. 2. The integrated angular deflection is less than 0.1 mrad and the integrated displacement of the jet is ~0.1 mm over the path. These deflections are sufficiently small that assumption that the jet travels in a straight path (ignoring gravity) is valid.

We have modeled this system using the ELEKTRA [5] time varying electromagnetic finite element program. This program solves the eddy current problem for a material with conductivity moving through a magnetic field. Figure 5 shows j_ϕ and j_z calculated at the outer surface of the mercury jet.

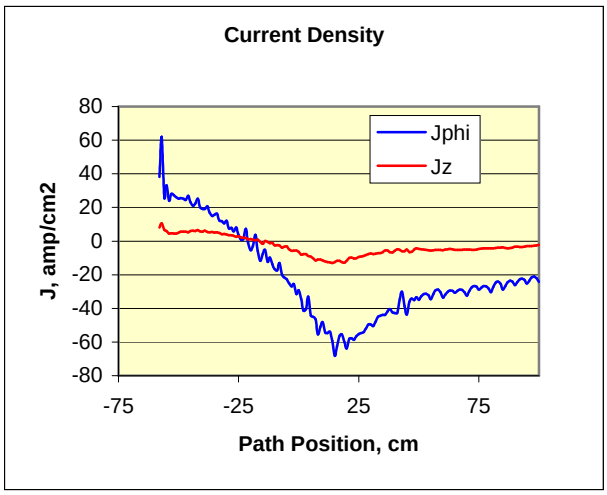

Figure 5: Induced j_ϕ and j_z from the finite element calculation along mercury jet path. The current densities are calculated on the surface of the jet.

4. ACKNOWLEDGEMENT

This work was supported by the US DOE under Contract No. DE-AC02-98CH10886.

5. REFERENCES

[1] *Feasibility Study-II of a Muon-Based Neutrino Source*, eds. S. Ozaki, R. Palmer, M. Zisman and J. Gallardo, BNL-52623 (2001).
[2] J. Gallardo et al., *First Order Perturbative Calculations for a Conducting Liquid Jet in a Solenoid.*
[3] K. McDonald, *An R&D Program for Targetry and Capture at a Muon Collider Source.* BNL E951 proposal.
[4] R. Weggel, *Behavior of Conducting Solid or Liquid Jet Moving in a Magnetic Field…*, BNL-65611.
[4] R. Samulyak, W. Oh and K.T. McDonald, *Numerical Simulation of Liquid Jets in Magnetic Fields and Applications*, (Apr 3, 2001).
[5] ELEKTRA is part of the Vector Fields Opera3D suite of electromagnetic computation programs. *Opera3D User's Manual*, VF-04-00-D2.